

An Introduction to Broadband Impedance Transformation for RF Power Amplifiers

By Anthony J. Bichler
RF Micro Devices, Inc.

This tutorial article reviews impedance matching principles and techniques, as they are applied to power device matching in amplifier circuits

This paper discusses broadband impedance-transforming techniques specific for radio frequency power amplifiers. Single and multiple Q matching techniques are demon-

strated for broadband performance; here the reader will understand the importance of a load impedance trajectory relevant to load pull contours.

Introduction

When analytically defining radio frequency circuits, a common approach incorporates admittance or impedance. Admittance, which is symbolized by Y , is defined in terms of conductance G and an imaginary susceptance component, jB . Admittance is often useful when defining parallel elements in a network and is expressed by the complex algebraic equation $Y = G + jB$.

Impedance, the mathematical inverse of admittance, is symbolized by Z and consists of a resistive component R in units of ohms and a reactive or imaginary component jX . Together in a series complex expression they define impedance as $Z = R + jX$. Impedance in this rectangular form is often used in industry to define a power device's optimal source or load.

For linear systems, the condition for maximum power transfer is obtained when the impedance of the circuit receiving a signal has an equal resistance and an opposite reactance of the circuit sending the signal. In the mathematics of complex variables, this relationship is known as the complex conjugate. The complex conjugate of a complex number is

obtained by simply reversing the sign of the imaginary part. Here Z^* denotes the complex conjugate of Z ; thus, for linear systems the condition for maximum power transfer is when $Z_{\text{Load}} = Z_{\text{Source}}^*$, or: $Z_L = Z_S^*$.

As the frequency of operation changes for Z_S , relative to its parasitics, the value of the resistive component can substantially change as well as the value of the imaginary component. Transforming a standard system impedance to present a driving point load impedance Z_L that maintains a complex conjugate relationship to the source impedance change over frequency is the most challenging aspect of broadband design.

Note: The linear condition for maximum power transfer is often traded for other performance parameters such as efficiency or gain. For this tradeoff the load impedance will not hold a conjugate relationship; however, the challenge of maintaining a load for this performance parameter over a broadband will generally remain the same.

A Review of Smith Chart Fundamentals

Philip H. Smith introduced the Smith Chart in *Electronics Magazine* on January 1939, revolutionizing the RF industry [1, 2]. This chart simplified complex parallel to series conversions graphically and, for the first time, provided intuitive transmission line solutions.

The Smith Chart is a graphical reflection coefficient system with normalized conformal mapping of impedance or admittance coordinates, as shown Figure 1 and 2, respectively. Reflection coefficient is often referred to as *gamma* and is symbolized by the Greek letter Γ . Gamma in its simplest form is defined as

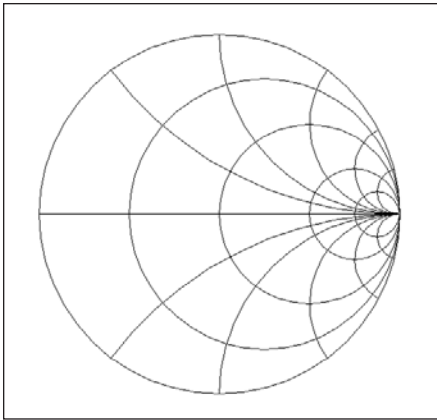


Figure 1 · The Impedance Smith Chart.

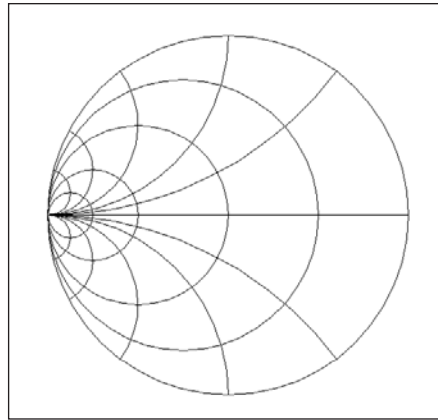


Figure 2 · The Admittance Smith Chart.

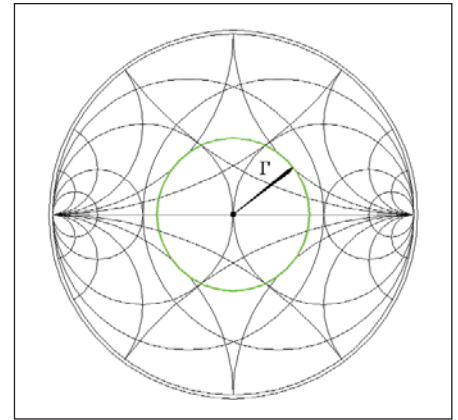


Figure 3 · The Immittance Chart with an SWR circle (green line) defined by (Γ) radius.

the ratio of the root of the incident power wave versus the root of the reflected power wave [3]:

$$\Gamma = \frac{\sqrt{W_r}}{\sqrt{W_i}}$$

where W_r is the reflected power and W_i is the incident power. Gamma can also be defined in terms of impedance where

$$\Gamma = \frac{Z_L - Z_S}{Z_L + Z_S}$$

For a large impedance mismatch Γ would approach unity, and for a near perfect match Γ would approach zero.

Impedances are often normalized when plotted on the Smith Chart. Normalizing Z_L to the center of the Smith Chart where $Z = 1$ gives one access to the chart's maximum resolution. Note that normalizing is the division of an impedance by a reference [4]. For example, normalizing with the 50-ohm system load impedance as the reference ($Z_0 = 50$), a source impedance of $Z_S = 100 + j50$ would normalize to $Z_S/Z_0 = 2 + j1 = z_s$, where the lower case z is used for normalized impedances. Most computer aided design or Smith Chart programs have simplified the normalization process. In the case of normalizing, the center of the chart

will conveniently reference to 50 ohms or another value as defined by the user.

The Smith Chart's horizontal centerline is known as the *resistive line*. It is scaled left to right, zero to infinity, with the normalized impedance (Z_0) centered in the middle of the chart. On the lower half of the chart below the resistive line, are the capacitive coordinates and above the line are the inductive coordinates. The circles that are tangent to the right side of the impedance Smith Chart are the circles of constant resistance. Above and below the right side at $R = \text{infinity}$ are the semicircles of constant reactance.

On the Admittance Smith Chart, the circles that are tangent to the left side are the circles of constant conductance and the semicircles above and below to the left where $R = 0$ are the circles of constant susceptance.

The Admittance Smith Chart is simply a mirror image of the Impedance Smith Chart where the Impedance Smith Chart can be rotated by 180 degrees to serve as an Admittance Chart. This duality of the Smith Chart is exploited for admittance to impedance conversions by simply rotating both the reflection coefficient vector by 180 degrees and then the chart itself by 180 degrees. Note that since the Smith Chart is a reflection system, 180 degrees around

the circumference is equivalent to 90 degrees of wavelength rotation.

A Smith Chart that has combined the Admittance and Impedance Smith Charts for simplicity is known as the Immittance Chart [5]. With the Immittance Chart a network consisting of capacitors or inductors in shunt or in series can be easily cascaded without rotating the chart.

In Figure 3, an Immittance Chart, the Gamma vector magnitude defines the radius of a constant standing wave ratio (SWR) circle. Standing waves are a phenomenon of the voltage or current waves from the summation of an incident power wave and reflected power wave on a transmission line from a mismatched load. SWR is the ratio of the maximum versus the minimum voltage or current on a standing wave and is commonly referred to as VSWR or ISWR, for voltage or current respectively. [6, 7]

SWR can be expressed in terms of Gamma's magnitude by

$$SWR = \frac{1 + |\Gamma|}{1 - |\Gamma|}$$

or directly by the mismatch impedances

$$SWR = \frac{Z_L}{Z_S}$$

or

$$SWR = \frac{Z_S}{Z_L}$$

where the equation choice is dictated by which one provides a quantity greater than unity.

SWR circles are used throughout the following Smith Chart illustrations to quantify the mismatch over frequency.

The Importance of Quality Factors

It is important to understand the quality factors Q , as they are integral to bandwidth. Q factors are used to define the quality of a reactive element by its ability to store energy, to fundamentally define bandwidth, and to define the ability of a loaded network to store energy. To ease some of the confusion with these Q factors they have been assigned the terms unloaded Q , loaded Q , and Q of the load respectively [8].

Unloaded Q is fundamentally defined as the ratio of stored energy versus dissipated energy [10] or

$$Q_{\text{Unloaded}} = \frac{\text{reactive power}}{\text{real power}} = \frac{I^2 X}{I^2 R}$$

which reduces to

$$Q_{\text{Unloaded}} = \frac{X}{R}$$

For capacitors, unloaded Q is expressed as a ratio of capacitive reactance to equivalent series resistance (ESR) [9] or

$$Q_{\text{Unloaded}} = \frac{X_C}{R_{\text{ESR}}}$$

and for inductors unloaded Q is expressed by

$$Q_{\text{Unloaded}} = \frac{X_L}{R}$$

where R is the series resistance from the windings of the coil.

Loaded Q is defined by the band's

center frequency (F_C) divided by the 3 dB bandwidth and is expressed as

$$Q_{\text{Unloaded}} = \frac{F_C}{BW}$$

For simple resonant tank networks, unloaded Q can be substituted with loaded Q in bandwidth calculations [11]. When the resonant frequency is equal to the center frequency, then unloaded Q can define the bandwidth by

$$BW = \frac{F_C}{Q_{\text{Unloaded}}}$$

or with substitution

$$BW = \frac{F_C}{X/R}$$

The Q of the load is often used to define a loaded network, which typically consists of ideal (lossless) matching elements. The network is not lossless since energy is propagated to and absorbed by the load. It is defined as before with the unloaded Q as a ratio of the reactance to resistance

$$Q = \frac{X}{R}$$

or in terms of vectors; the imaginary component magnitude versus the resistive component.

Plotting Q of the load as constant ratio on the Smith Chart will define a constant Q curve. These Q curves are often used as guideline boundaries for broadband transformations and will be used throughout the following illustrations to define the transforming networks. As a rule in broadband transformations, maintaining a lower Q curve for a given transformation by increasing the number of n-sections will yield a higher bandwidth.

For a single section transformation where the resistive line and a constant Q of the load curve bound the transformation, the relationship between the Q of the load and the

resistive transformation ratio is given by [12]

$$1 + Q^2 = R_{\text{ratio}}$$

For increasing bandwidth by increasing the number of n-sections having equal Q the relationship becomes

$$1 + Q^2 = \left(\sqrt[n]{R_{\text{ratio}}}\right)$$

Note: Using the guideline boundaries above in this reference does not yield the optimal broadband design. Other topologies will be discussed such as the Chebyshev response transformation, which has a significant bandwidth advantage over the single Q matching technique. Single Q advantages to be considered are transformation efficiency with smaller component values and design simplicity.

In practice using more than a four-section matching network will not yield greater bandwidth.

Also, Q of the load should not be substituted with unloaded Q or loaded Q . For example, in the following multiple section illustrations, which are bounded by a Q of the load curve = 1.75 (for a 50 to 3 ohm transformation), yield more 3 dB bandwidth than defined by the loaded Q of 1.75.

Q of the load will be referred to throughout the remainder of this discussion as the single letter Q .

Computer-Aided Design (CAD) and Other Smith Chart Programs

Smith Chart programs such as the early Motorola Impedance Matching Program (MIMP) provide a useful tool by automating the repetitive graphical computations [13]. Considering the frequency point calculations required for resolution of a broadband matching network, this is a tedious task at best. Smith Chart programs quickly and accurately plot the required trajectories and circles allowing the designer to focus on the design and not the mechanics of generating a display. Other Smith Chart

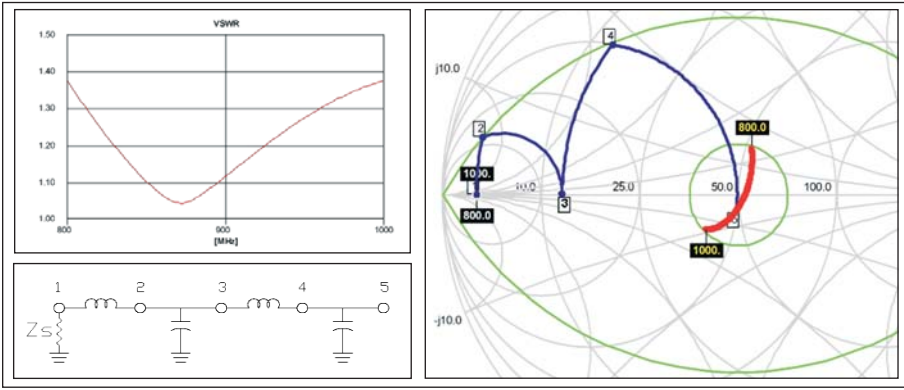


Figure 4 · $Z_0 = 50$, $Z_S = 3$, $Q = 1.75$, $SWR = 1.4$; N1-2 Series $L = 0.9$ pH, N2-3 Shunt $C = 25$ pF; N3-4 Series $L = 3.8$ nH, N4-5 Shunt $C = 6.5$ pF.

programs followed MIMP such as winSmith [14], LinSmith [15], and Smith32 [16]. Although these programs leveraged an engineer’s intuitive creativity with symmetrical Q matching solutions, they fall short of the sophistication that CAD systems provide. Systems such as Applied Wave Research’s Microwave Office [17] and Agilent’s Advanced Design System (ADS) [18] offer electromagnetic simulation of arbitrary structures, complex network synthesis, and optimizers that provide a fully automated solution. Modern CAD systems now offer a complete simulation toolset with non-linear synthesis and layout functions.

When the design challenge is more fundamental, and when the best solution is intuitively derived, Smith Chart programs are well suited for the task. The following demonstrations were plotted with the author’s preference, Smith32.

Transformation and Performance

Figure 4 illustrates a 2-section (4-element) transformation from a 3-ohm driving point impedance to a 50-ohm load, a 16.7:1 transformation ratio. Confined to a constant $Q = 1.75$ curve and the resistive line, the Gamma from the 800 - 1000 MHz trajectory (in red) is quantified with a SWR circle of 1.4 (center green circle).

To predict the performance response from the trajectory, the

transformation is reversed. Transforming from the 50-ohm system impedance the load trajectory is illustrated relative to a laterally diffused metal oxide semiconductor device (LDMOS) load pull performance contours in Figure 5.

The trajectory intersects several contours in gain and linearity; however, the contours represent performance for single frequency operation (2-tone 880 MHz). These contours will follow a trajectory of their own relative to the parasitic capacitance of an LDMOS device. Moreover and important to note, the trajectory of these contours will track opposite (counterclockwise) to the driving point load trajectory thus further degrading broadband performance.

Figure 6 illustrates a model of a LDMOS power amplifier with plotted complex conjugate load impedance points at 800 MHz, 900 MHz, and 1000 MHz. For this model, load pull contours would track counterclockwise as with the indicated conjugate trajectory points [4]. An ideal counterclockwise load trajectory would be a challenge to any broadband designer; the popular compromise is a compressed and or folded trajectory design.

The optimal output load impedance of RF transistors as generally published in manufacture data sheets includes all capacitive and package lead parasitics. In the absence of this

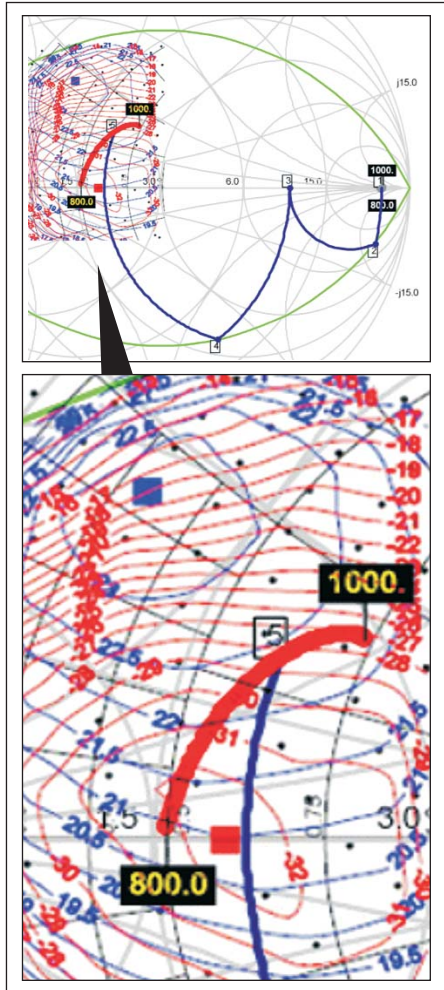


Figure 5 · Trajectory relative to 60W_{PEP} LDMOS Load Pull contours (19): $Z_0 = 3$, 28V_{DC}, 900 MHz; Max Gain = 23.6 dB @ $Z = 1.0 + j1.3$; Min IMD3 = -32.7 dBc @ $Z = 1.0 + j0.0$; Max Eff = 66.75% @ $Z = 0.9 + j1.8$.

data or when the data sheet is not applicable to the design an approximation can be derived [20].

The purely resistive component of the optimal load (RL) can be approximated from the operational RF output power and supply voltage from the equation

$$R_L = \frac{V^2}{2P_{out}}$$

With the transistor biased off the output parasitic capacitance can then be measured directly with a capaci-

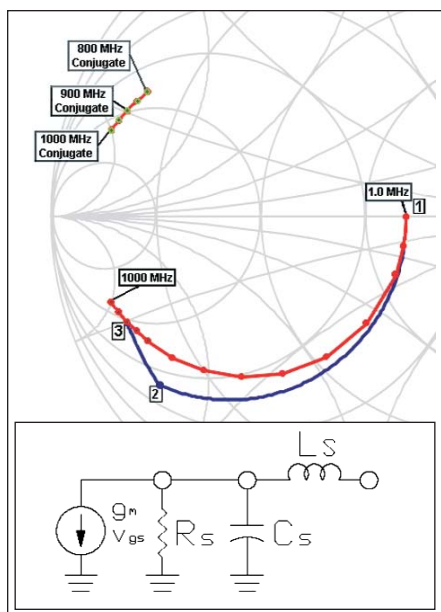


Figure 6 · A simple LDMOS model with indicated complex conjugate loads: $Z_0 = 5$, $R_L = R_S = 13$, $C_S = 47.5$ pF, $L_S = 250$ pH.

tance meter. The output inductance can be derived from package and wire-bond mechanical dimensions.

In this packaged 28V, 30W, LDMOS model

$$R_{S \text{ Model}} = R_L = 28^2 / 2(30) = 13\Omega$$

For 900 MHz the capacitive parasitic (C_S) and lead inductance (L_S) transform $R_{S \text{ Model}}$ to $Z_{S \text{ Model}} = 1 - 2j$

Other transistor technologies such as gallium arsenide (GaAs) and gallium nitride (GaN) have greatly reduced capacitance for broadband performance. For example RFMD's GaN1C process having higher current density is only 0.05 - 0.1 pF/W where LDMOS has roughly 0.75 pF/W of output capacitance. The bandwidth achievable is highest for the GaN followed by GaAs, and LDMOS. The tradeoff of the lower capacitance technologies is monetary with LDMOS having the best economical value.

Transformation with the Low-Pass L-Network

For standardization and uniformi-

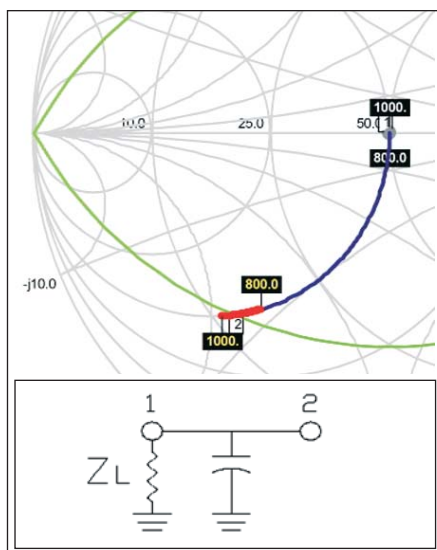


Figure 7 · $Z_0 = 50$, $Q = 1.75$; N1-2 Shunt C = 6 pF.

ty, the following transformations are confined to a <25% fractional bandwidth (800 MHz to 1000 MHz) with 900 MHz set as the reference.

In Figure 7 shunt capacitance rotates the trajectory clockwise from $Z_L = 50$ with increasing frequency or with capacitance value following the admittance equation

$$jB_C = j\omega C = \frac{1}{jX_C}$$

Note the trajectory from 800 MHz to 1000 MHz (in red) is co-angular with the shunt capacitive reactance (in blue) following the constant conductance circle.

In Figure 8, series inductance rotates the trajectory clockwise along a constant resistance circle with increasing frequency or with an increase of inductance following the reactance equation

In summary, shunt C and series L disperse a trajectory with increasing frequency. In other words when using these matching elements in a low-pass network, the higher frequencies will rotate and transform more than the lower frequencies, which spreads the trajectory relative to frequency in a clockwise direction.

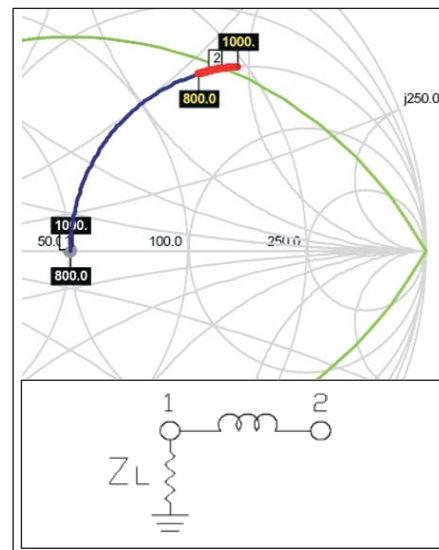


Figure 8 · $Z_0 = 50$, $Q = 1.75$; N1-2 Series L = 15nH.

In Figure 9 a two-element low-pass network is charted on a $Z_0 = 25$ normalized Smith Chart. The normalized impedance of 25 ohms is calculated from the geometric mean of the system load and source impedance, 50 to 12.5 ohms respectively [5].

$$Z_{Geo} = \sqrt{Z_L * Z_S}$$

The constant Q curve of 1.75 is derived from the resistive ratio of 50/12.5 from the equation

$$1 + Q^2 = R_{ratio}$$

Note that the impedance trajectory is no longer co-angular to the constant resistance arc of the series inductance reactance (nodes 2-3).

High-Pass Lumped Elements and the High-Pass L-Network

Shunt inductive reactance as demonstrated in Figure 10 rotates clockwise along a constant conductance circle with increasing frequency following the susceptance equation

$$jB_L = \frac{1}{jX_L} = \frac{1}{j\omega L}$$

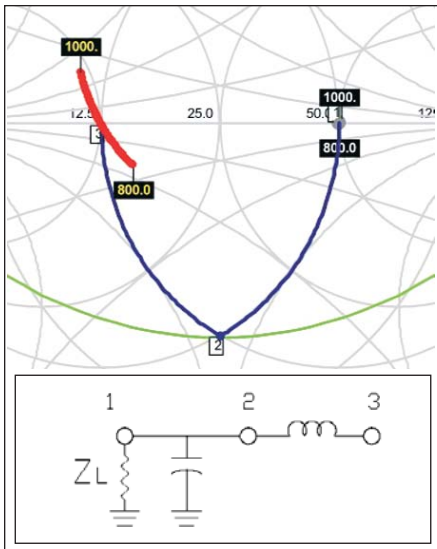


Figure 9 · $Z_0 = 25$, $Q = 1.75$; N1-2 Shunt $C = 6.1$ pF; N2-3 Series $L = 3.8$ nH.

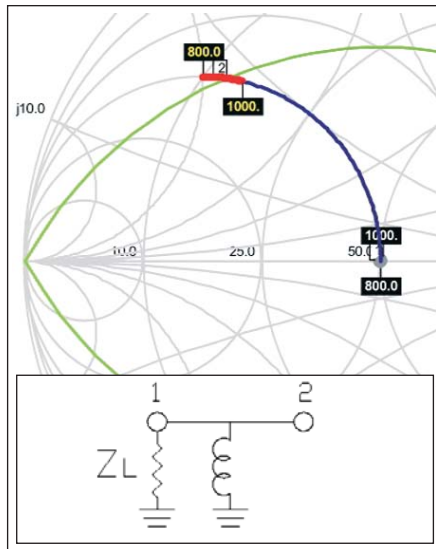


Figure 10 · $Z_0 = 50$, $Q = 1.75$; N1-2 Shunt $L = 5$ nH.

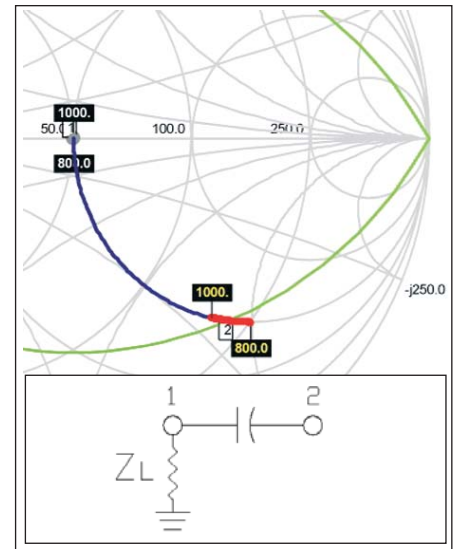


Figure 11 · $Z_0 = 50$, $Q = 1.75$; N1-2 Series $C = 2$ pF.

This element is different than the two matching elements discussed previously such that shunt inductance susceptance decreases with increasing frequency.

Series capacitance is similar; however, its reactance is plotted on a constant resistance circle in Figure 11 following the reactance equation

$$jX_C = \frac{1}{j\omega C}$$

Series capacitive reactance rotates clockwise with increasing frequency and decreases with increasing frequency.

Shunt L and series C disperse an impedance trajectory in a clockwise direction with frequency, but the reactance will be decreasing with frequency. Hence, high-pass matching networks consisting of shunt inductors and series capacitors will transform the lower frequencies more than the higher frequencies.

In Figure 12, a two-element high-pass L-network transformation from 50 to 12.5 ohms is demonstrated on a 25-ohm normalized Smith Chart. Note that the trajectory is no longer co-angular to the constant resistance circle of (nodes 2-3) and that unlike a

low-pass L -network, the higher frequencies are transformed less than the lower frequencies. If the low-pass trajectory of Figure 9 were overlaid onto Figure 12, the two trajectories would form the letter X. Exploiting this relationship by combining these dispersion effects can leverage a broadband transformation.

Compressing Trajectory Dispersion

A broadband band-pass network is illustrated in Figure 13, a 50 to 3 ohm transformation similar to the one in Figure 4. With the Smith Chart normalized to the geometric mean, it is easy to see that low pass nodes 1-2-3 are symmetrical in Q to the high pass nodes 3-4-5. Combining these two networks' halves folds and compresses the trajectory into a condensed 3-ohm driving point load.

Compare this transformation, which has a mismatch SWR of 1.08, to that of Figure 4 where the mismatch SWR is 1.4.

A Chebyshev broadbanding technique is illustrated in Figure 14. As discussed earlier, when using low-pass networks the higher frequencies transform and rotate more. Here the frequencies higher than 800 MHz are

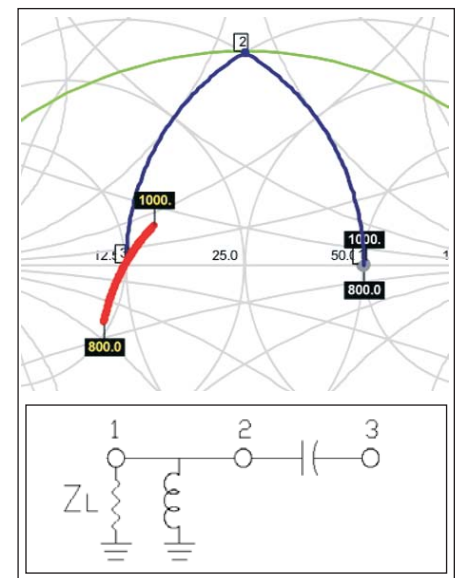


Figure 12 · $Z_0 = 25 \Omega$, $Q = 1.75$; N1-2 Shunt $L = 5.1$ nH; N2-3 Series $C = 8.2$ pF.

over-rotated well beyond the resistive line at node 3, which compresses the upper frequency dispersion. Again, compare this network of Figure 14 to that of Figure 4; a 3-ohm SWR bandwidth of 1.12 versus 1.4.

The transformation is mostly symmetrical with two Q curves, an outer curve (Q_1 green) and an inner curve (Q_3 magenta). However, node 5

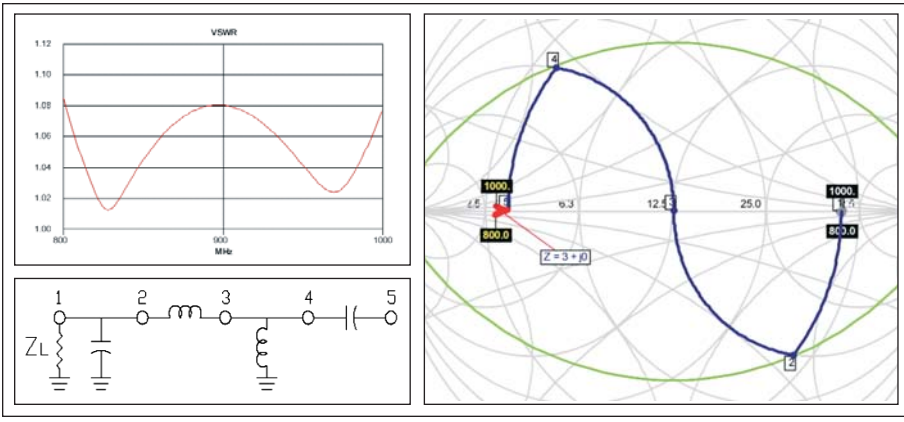


Figure 13 · 50 to 3-ohm transformation; $Z_0 = 12.5$, $Q = 1.75$; N1-2 Shunt C = 6.10 pF; N2-3 Series L = 3.85 nH; N3-4 Shunt L = 1.32 nH; N4-5 Series C = 32.3 pF.

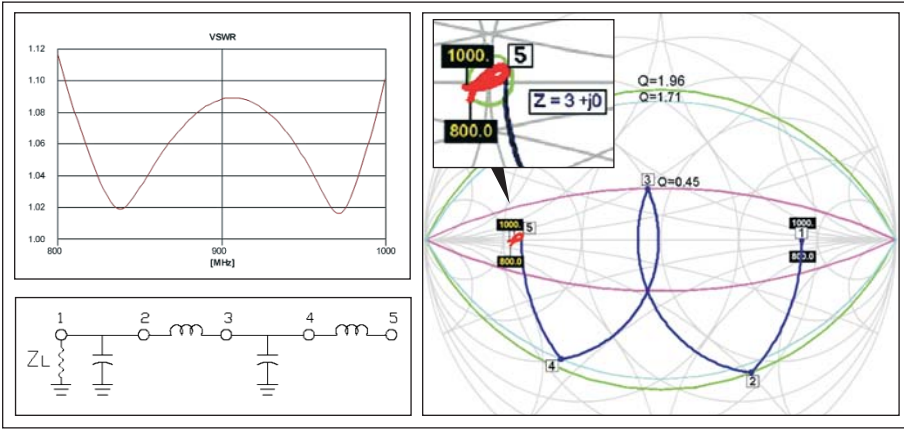


Figure 14 · $Z_0 = 12.3$, SWR = 1.12 @ $Z_s = 3$; N1-2 Shunt C = 6.9 pF; N2-3 Series L = 4.4 nH; N3-4 Shunt C = 30.4 pF; N4-5 Series L = 0.99 nH.

falls at a higher impedance than the 3-ohm target to center the fish shaped trajectory at $Z = 3 + j0$ and so therefore a third Q curve (Q_2 , cyan) is defined at node 4.

With the complexity of the multiple Q curve network, deriving a design from a Smith Chart alone would not be an intuitive process. The Q curves are in overlapping fractions of the resistive transformation and do not hold the relationship with the transformation ratio as before with single Q networks. This network and Tables 1 and 2 were derived by optimization with an ADS simulator utilizing a gradient optimizer.

Note that the inner Q curve (Q_3) as a function of the transformation ratio holds an inverse relationship to

that of the other Q curves.

In Figure 15, a three-section transformation, the trajectory fits into a 3-ohm 1.01 SWR circle. Three Q curves are adequate for defining the three section network since the trajectory is small and circular in shape, unlike in Figure 14; here no impedance offset is needed at node 7.

As mentioned above, Table 2 was derived from optimization. Here Q curves are provided for resistive transformation ratios of 1.67:1 (50 ohms to 30 ohms) to 100:1 (50 ohms to 0.5 ohms).

Complex Transformations

All transformations discussed previously have been purely resistive to resistive (50-ohm to 3-ohm) trans-

| Q_1 | Q_2 | Q_3 | Trans Ratio |
|-------------|-------------|-------------|--------------|
| 0.72 | 0.71 | 0.61 | 1.67 |
| 0.82 | 0.80 | 0.62 | 2.0 |
| 1.27 | 1.22 | 0.58 | 5.0 |
| 1.63 | 1.51 | 0.50 | 10.0 |
| 1.96 | 1.71 | 0.45 | 16.67 |
| 2.19 | 1.91 | 0.42 | 25.0 |
| 2.39 | 2.01 | 0.38 | 33.3 |
| 2.72 | 2.15 | 0.35 | 50 |
| 3.30 | 2.53 | 0.29 | 100 |

Table 1 · Q curves per transformation ratio (2-section network). The Q curves are numbered from the outer most Q_1 towards the inner Q_3 .

| Q_1 | Q_2 | Q_3 | Trans Ratio |
|-------------|-------------|-------------|--------------|
| 0.92 | 0.60 | 0.65 | 1.67 |
| 1.37 | 0.90 | 0.61 | 5.00 |
| 1.53 | 1.00 | 0.60 | 7.14 |
| 1.68 | 1.08 | 0.58 | 10.00 |
| 1.89 | 1.21 | 0.53 | 16.67 |
| 2.06 | 1.32 | 0.50 | 25.00 |
| 2.20 | 1.41 | 0.49 | 33.33 |
| 2.41 | 1.52 | 0.45 | 50.00 |
| 2.57 | 1.61 | 0.44 | 66.67 |
| 2.80 | 1.74 | 0.41 | 100.00 |

Table 2 · Q curves per resistive transformation ratio (3-section network). The Q curves are numbered from the outer most Q_1 towards the inner Q_3 .

formations. Figure 16 demonstrates an immediate approach to a high Q transformation from a purely resistive impedance of $Z_0 = 50$, to a load impedance with where $Z_L = 20 + j50$.

A broadband match in this case is seemingly impossible to design, especially when considering the source impedance dispersion from the large corresponding parasitics. However, the transformation can be forbearing; Figure 17 includes an additional

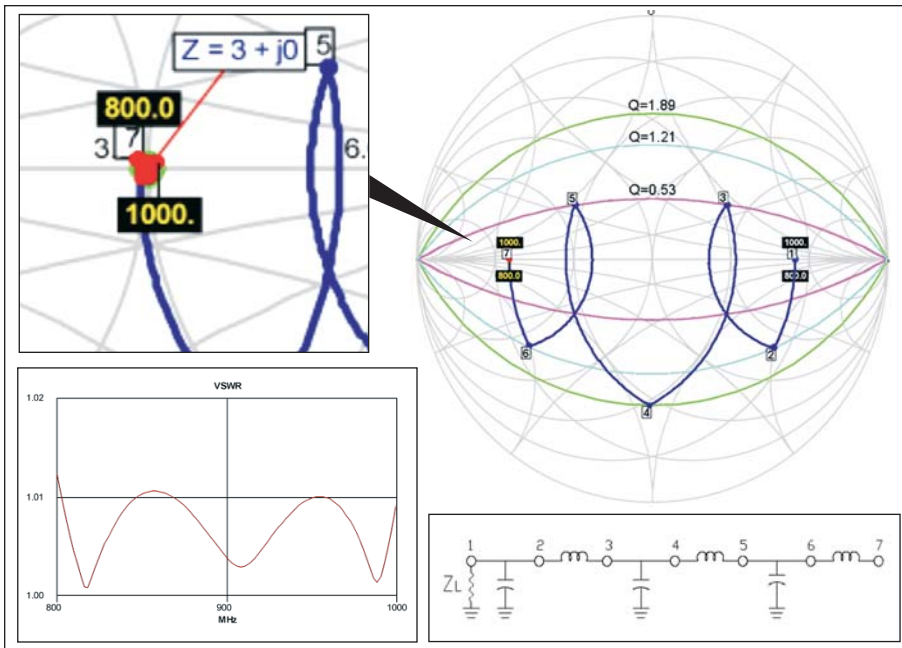


Figure 15 · $Z_0 = 12.2$, SWR = 1.01 @ $Z_S = 3$; N1-2 Shunt C = 4.30 pF, N2-3 Series L = 6.22 nH; N3-4 Shunt C = 16.57 pF, N4-5 Series L = 2.42 nH; N5-6 Shunt C = 42.05 pF, N6-7 Series L = 0.63 nH.

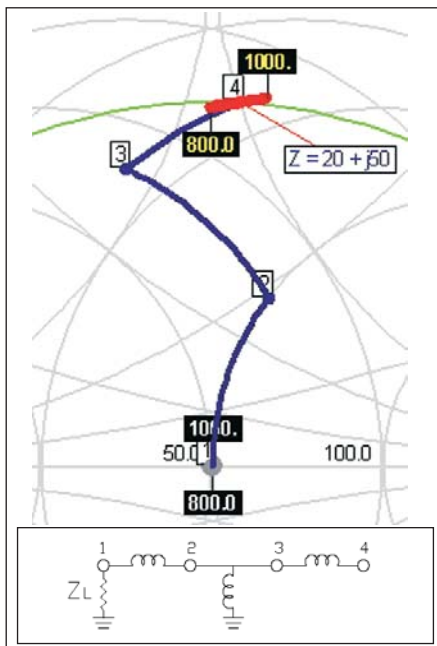


Figure 16 · $Z_0 = 50 \Omega$, $Q = 2.5$.

shunt capacitor that is proportioned for the complex target impedance. This additional element re-orders the dispersion effects of the transforming network; hence improving broadband performance. It is another example of

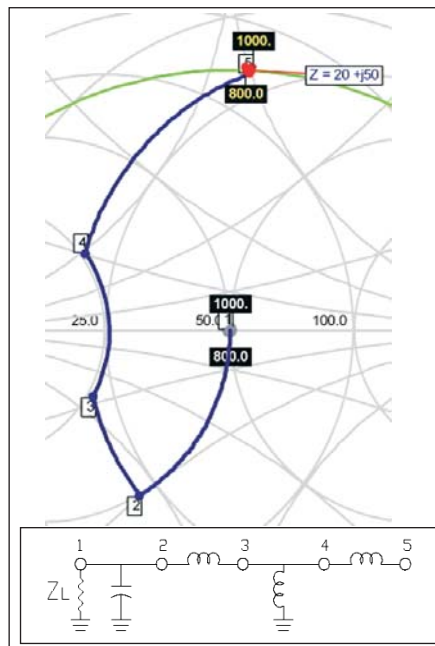


Figure 17 · $Z_0 = 50 \Omega$, $Q = 2.5$; N1-2 Shunt C = 4.0 pF, N2-3 Series L = 2.8 nH; N3-4 Shunt L = 5.0 nH, N4-5 Series L = 7.0 nH.

how the dispersion effects from lumped elements can be leveraged to compress and fold the trajectory.

Conclusion

Multiple frequency point load pull contours demonstrate the necessity for a compressed and/or folded impedance trajectory for optimized broadband power amplifier design. Single Q matching where the resistive line and Q curve serve as guideline boundaries are too often presented as the mainstream broadband design technique. Here we have shown that multiple Q curve transformations although more complex in their derivation have superior bandwidth over the single Q matching technique although the single Q matching technique is easily demonstrated we recommend that designers consider a multiple Q transformation. Furthermore, where device and package parasitics disperse the source impedance counter to a broad band transformation, the use of multiple Q curve transformations is perhaps a categorical.

Acknowledgements

The author is indebted to many friends who reviewed this document for accuracy.

Special thanks to John B Call for many broadband network discussions. Special thanks to Kal Shallal for the LDMOS load pull contours, and for the device modeling discussion.

References:

1. "Philip H. Smith: A Brief Biography" by Randy Rhea, Noble Publishing 1995.
2. Smith® Chart is a registered trademark and is the property of Analog Instrument Company, New Providence, NJ.
3. Michael Hiebel, Fundamentals of Vector Network Analysis, Rohde & Schwarz 2007, pg. 14.
4. Chris Bowick, *RF Circuit Design*, Newnes imprint of Butterworth-Heinemann, 1982, Ch. 4 - 5.
5. Herbert L. Krauss, Charles W. Bostian, Fredrick H. Raab, *Solid State Radio Engineering*, Zhuyi

Publishing of Taiwan 1980.

6. Donslf W. Dearholt, William R. McSpadden, *Electromagnetic Wave Propagation*, McGraw-Hill Inc. 1973 , Ch. 5.4 - 5.5.

7. Joseph F. White, *High Frequency Techniques / An Introduction to RF and Microwave Engineering*, John Wiley & Sons 2004.

8. Randy Rhea, "Yin-Yang of Matching: Part 2- Practical Matching Techniques," *High Frequency Electronics*, April 2006.

9. *The RF Capacitor Handbook*, American Technical Ceramics Corp. 1994.

10. *1989 ARRL Handbook for the Radio Amateur*, American Radio Relay League, pp 2-27 thru 2-29.

11. Thomas L. Floyd, *Electronics Fundamentals: Circuits, Devices, and Applications*, 2nd ed. McMillan Publishing Co. 1991, Chapters 14.4 - 14.7

12. J. F. White, *High Frequency Techniques / An Introduction to RF and Microwave Engineering*, John Wiley & Sons 2004, pp. 70-71.

13. Dan Moline, *Motorola Impedance Matching Program*, Motorola Inc., April 6, 1992.

14. Agilent Technologies, win-Smith 2.0, Noble Publishing 1998.

15. linSmith, John Coppens, 1999-2008, www.jcoppens.com/soft/linsmith.

16. Pederson, Ib F., Smith32, Denmark 2002.

17. Applied Wave Research, Inc. Microwave Office®, El Segundo, CA.

18. Agilent Technologies, Advanced Design System.

19. Load Pull contours courtesy of Khalid Shallal, RFMD.

20. B. Becciolini, *Impedance Matching Networks Applied To R-F Power Transistors*, Motorola AN-721, Motorola Inc., 1974.

Author Information

Anthony Bichler is a design engineer with RFMD in Chandler Arizona. His 25 years of RF experience includes power amplifier design for RFID, cellular handsets, and base stations. Presently,



Tony is working on quad-band transmit modules for GSM, PCS, and DCS handsets. Interested readers may contact him at tbichler@rfmd.com

Article Archives

Remember, all of our technical articles and columns are available as PDF files for download from our Web site!

Articles in the current print and Online Edition become available in the Archives upon publication of the next issue.

HIGH FREQUENCY

ELECTRONICS

www.highfrequencyelectronics.com